



Role of spatial modes in Hermite-sinh-Gaussian beams with radial polarization for electron acceleration in vacuum

Vivek Sharma^{1,2} and Vishal Thakura*

¹ Department of Physics, Lovely Professional University, G.T. Road, Phagwara, Punjab, India

² Department of Physics, Ch. Balluram Godara Government Girls College, Sri Ganganagar, Rajasthan, India

E-mail: vishal20india@yahoo.co.in

(Received 31 July 2025 ; in final form 15 October 2025)

Abstract

This paper investigates the potential of Hermite-sinh-Gaussian (HSG) laser beams to improve the efficacy of electron acceleration in vacuum. HSG beams are distinguished by their hybrid structure, which encompasses Hermite-Gaussian orthogonality and non-Gaussian characteristics introduced by the hyperbolic sine (sinh) function. This structure provides distinctive capabilities for the manipulation of laser electric fields. The study examines the responsibilities of critical parameters, such as the Hermite mode index (s), the decentered parameter (b) of the sinh function, and the electric field amplitude and distribution, in the optimization of electron acceleration dynamics. The interplay between these parameters and their effect on energy gain and trajectory confinement is analyzed using theoretical modelling and numerical simulations. The results indicate that the maximum total energy can be enhanced to 3375.75 MeV by customized HSG beam configurations ($s = 2, b = 3$), which can provide valuable insights for the development of advanced laser-driven particle accelerators. These results facilitate the development of compact, high-efficiency electron acceleration technologies that have applications in radiation generation and particle physics.

Keywords: Radial polarized Hermite-sinh-Gaussian laser, Decentered parameter, Hermite mode index, Electron energy gain, Energy efficiency.

1. Introduction

The prospective applications of electron acceleration in vacuum using high-intensity laser beams in particle physics, advanced radiation sources, and compact accelerator technology have made it a promising area of research. Significant advantages are provided in terms of the acceleration process's simplicity and control by the capacity to accomplish high electron energy gains through laser-electron interaction in plasma and vacuum. Structured laser fields have garnered attention for their capacity to optimize acceleration efficacy and manipulate particle trajectories, despite the presence of a variety of laser beam configurations.

Hermite-Gaussian (HG) laser pulse profile has been investigated in various phenomena like electron wave excitation [1,2] electron acceleration [3,4] self-focusing [5,6], THz generation [7,8] etc. Pramanik et al. [9] has investigated electron acceleration phenomenon in vacuum using Hermite-cosh-Gaussian laser pulse. Midha et al. [10] has investigated mode index of Hermite polynomial and decentered parameter of cosh function while investigating the THz generation efficiency using Hermite-cosh-Gaussian laser profile in plasma. Sinh-Gaussian and high order sinh Gaussian laser pulse has

been investigated in various laser-based applications [11], [12].

In this context, Hermite-sinh-Gaussian (HSG) laser beams offer a distinctive framework for the investigation of novel acceleration mechanisms. Hermite-Sinh-Gaussian beams are a composite laser mode that combines the orthogonality of HG beams with the hyperbolic sine (Sinh) function. They are characterized by their intricate transverse intensity profiles. The spatial distribution of the laser electric field is precisely controlled by this distinctive structure, which has a direct impact on electron dynamics. The spatial intensity and phase profile of the beam are significantly influenced by the Hermite mode index and the decentered parameter associated with the sinh function, which in turn influences the electron acceleration process. Tian et al. [13] has investigated the self-focusing effect of Hermite-sinh-Gaussian laser beam in plasma.

The experimental generation of Hermite sinh-Gaussian (HSG) beams, especially those with high mode indices (e.g., $s=2$), poses several notable challenges. The intricate field structure of HSG beams, defined by the hyperbolic sine function and modulated by Hermite polynomials, necessitates accurate amplitude and phase shaping. High

mode indices enhance sensitivity to misalignments and optical aberrations, thereby complicating beam formation and propagation. Achieving precise control over the beam parameter b , which influences the beam's non-Gaussian characteristics, presents challenges due to the requirements for high-resolution modulation and rigorous calibration. The scalability is constrained by the beam profile's sensitivity to environmental factors; while vacuum conditions mitigate scattering and absorption, their maintenance introduces operational complexity. Furthermore, accurate beam alignment is critical; minor deviations can compromise modal purity and result in energy loss or spatial decoherence.

The laser electric field is of the utmost importance in accelerating electrons [14,15]. The maximal energy gain that can be achieved is determined by the amplitude of the electric field, while the trajectory and confinement of electrons within the accelerating region are influenced by the field's spatial distribution. It is feasible to optimize the interaction between the laser field and the electron by adjusting the parameters of Hermite-sinh-Gaussian beams. This optimization has the potential to result in a more efficient acceleration and a greater transfer of energy to the electron.

This research examines the potential of Hermite-sinh-Gaussian laser beams for the high-efficiency acceleration of electrons in vacuum. The intensity profile of such a HSG laser pulse is shown in figure 1. We investigated the influence of the laser electric field, the decentered parameter of the sinh function, and the Hermite mode index on the acceleration dynamics. Our objective is to offer insights into the ways in which these parameters can be customized to optimize energy gain and enhance the overall efficiency of the electron acceleration process by means of the theoretical modelling presented in section II and the numerical simulations presented in section III. These insights are further elaborated upon in the conclusion section IV.

2. Electron dynamics

The general form of the electric field vector of a Hermite-sinh-Gaussian laser beam that is radially polarized and is travelling along the z-direction is described as

$$\vec{E} = E_r \hat{r} + E_z \hat{z} \quad (1)$$

Here, E_r and E_z are the components of electric field vector.

Like Hermite-cosh-Gaussian laser pulse [16], the radial component of the electric field of a spatial Hermite-Sinh-Gaussian laser beam can be written as

$$\vec{E}_r(r, z) = \hat{r} E_0 H_s \left(\frac{\sqrt{2}r}{r_0} \right) \sinh \left(\frac{br}{r_0} \right) e^{-\left(r^2/r_0^2\right)} e^{i(kz - \omega t)} \quad (2)$$

Here, E_0 is the amplitude of laser electric field, r_0 is the beam waist, s is Hermite polynomial mode index, b is decentered parameter associated with sinh function, k and ω are the propagation constant and frequency of laser pulse.

By solving Maxwell's first equation in vacuum $\frac{1}{r} \frac{\partial}{\partial r} [r E_r] + \frac{1}{r} \frac{\partial}{\partial \phi} [E_\phi] + \frac{\partial E_z}{\partial z} = 0$, for the chosen electric field as defined in equation (2), the z-component of electric field [17], [18] is

$$E_z = \frac{i E_r}{kr} \left[1 + 2\sqrt{2} s \left(\frac{r}{r_0} \right) \frac{H_{s-1} \left(\frac{\sqrt{2}r}{r_0} \right)}{H_s \left(\frac{\sqrt{2}r}{r_0} \right)} + \frac{rb}{r_0} \coth \left(\frac{br}{r_0} \right) - \frac{2r^2}{r_0^2} \right] \quad (3)$$

By solving Maxwell's third equation in vacuum $\vec{\nabla} \times \vec{E} = -\frac{\partial \vec{B}}{\partial t}$, magnetic field associated with the laser pulse is $\vec{B}_L = \frac{E_r}{c} \hat{\theta}$ (4)

$$\text{By taking components of the Lorentz force equation } \vec{F} = \frac{d\vec{p}}{dt} = -e \{ \vec{E} + (\vec{V} \times \vec{B}) \} \quad (5)$$

$$\text{Along radial direction } \frac{dP_r}{dt} = -e \left\{ E_r - \frac{V_z E_r}{c} \right\} \quad (6)$$

$$\text{Along z- direction } \frac{dP_z}{dt} = -e \left\{ E_z + \frac{V_r E_r}{c} \right\} \quad (7)$$

$$\text{Along } \Theta\text{-direction } \frac{dP_\theta}{dt} = 0 \quad (8)$$

As, Differentiating the formula of relativistic factor $\gamma = \sqrt{1 + \frac{P^2}{m_0^2 c^2}}$, we get

$$\frac{dy}{dt} = -\frac{e}{m_0 c^2} (V_r E_r + V_z E_z) \quad (9)$$

By using the values of laser electric and magnetic field components from equation (2-4), and normalizing the parameters as [17]

$$\begin{aligned} t' = \omega t, a_0 = \frac{e E_0}{m_0 c \omega}, \beta_r = \frac{V_r}{c}, \beta_z = \frac{V_z}{c}, r' = \frac{r \omega}{c}, r_0' \\ = \frac{r_0 \omega}{c}, k' = \frac{k c}{\omega}, z' = \frac{z \omega}{c}, \phi \\ = t' - k' z' \end{aligned}$$

We get,

$$\begin{aligned} \Rightarrow \frac{dy}{dt'} = \\ -a_0 H_s \left(\frac{\sqrt{2}r'}{r_0'} \right) \sinh \left(\frac{br'}{r_0'} \right) e^{-r'^2/r_0'^2} \left(\beta_r \cos(\phi) + \right. \\ \left. \sin(\phi) \frac{\beta_z}{k' r'} \left\{ 1 + 2\sqrt{2} s \left(\frac{r'}{r_0'} \right) \frac{H_{s-1} \left(\frac{\sqrt{2}r'}{r_0'} \right)}{H_s \left(\frac{\sqrt{2}r'}{r_0'} \right)} + \right. \right. \\ \left. \left. \frac{b r'}{r_0'} \coth \left(\frac{b r'}{r_0'} \right) - \frac{2r'^2}{r_0'^2} \right\} \right) \end{aligned} \quad (10)$$

Solving equation (6) in similar manner, we get

$$\frac{d\beta_r}{dt'} = -\frac{a_0}{c_1} H_s \left(\frac{\sqrt{2}r'}{r_0'} \right) \sinh \left(\frac{br'}{r_0'} \right) e^{-r'^2/r_0'^2} \cos(\phi) (1 - \beta_z) \quad (11)$$

$$\text{Here, } c_1 = \left\{ \frac{1}{\sqrt{1-\beta_r^2}} + \frac{\beta_r^2}{(1-\beta_r^2)^{3/2}} \right\}$$

Solving equation (7) in similar manner, we get

$$\begin{aligned} \frac{d\beta_z}{dt'} = -\frac{a_0}{c_2} H_s \left(\frac{\sqrt{2}r'}{r_0'} \right) \sinh \left(\frac{br'}{r_0'} \right) e^{-r'^2/r_0'^2} \left\{ \beta_r \cos(\phi) - \right. \\ \left. \frac{1}{k' r'} \sin(\phi) \left\{ 1 + 2\sqrt{2} s \left(\frac{r'}{r_0'} \right) \frac{H_{s-1} \left(\frac{\sqrt{2}r'}{r_0'} \right)}{H_s \left(\frac{\sqrt{2}r'}{r_0'} \right)} + \right. \right. \\ \left. \left. \frac{b r'}{r_0'} \coth \left(\frac{b r'}{r_0'} \right) - \frac{2r'^2}{r_0'^2} \right\} \right\} \end{aligned} \quad (12)$$

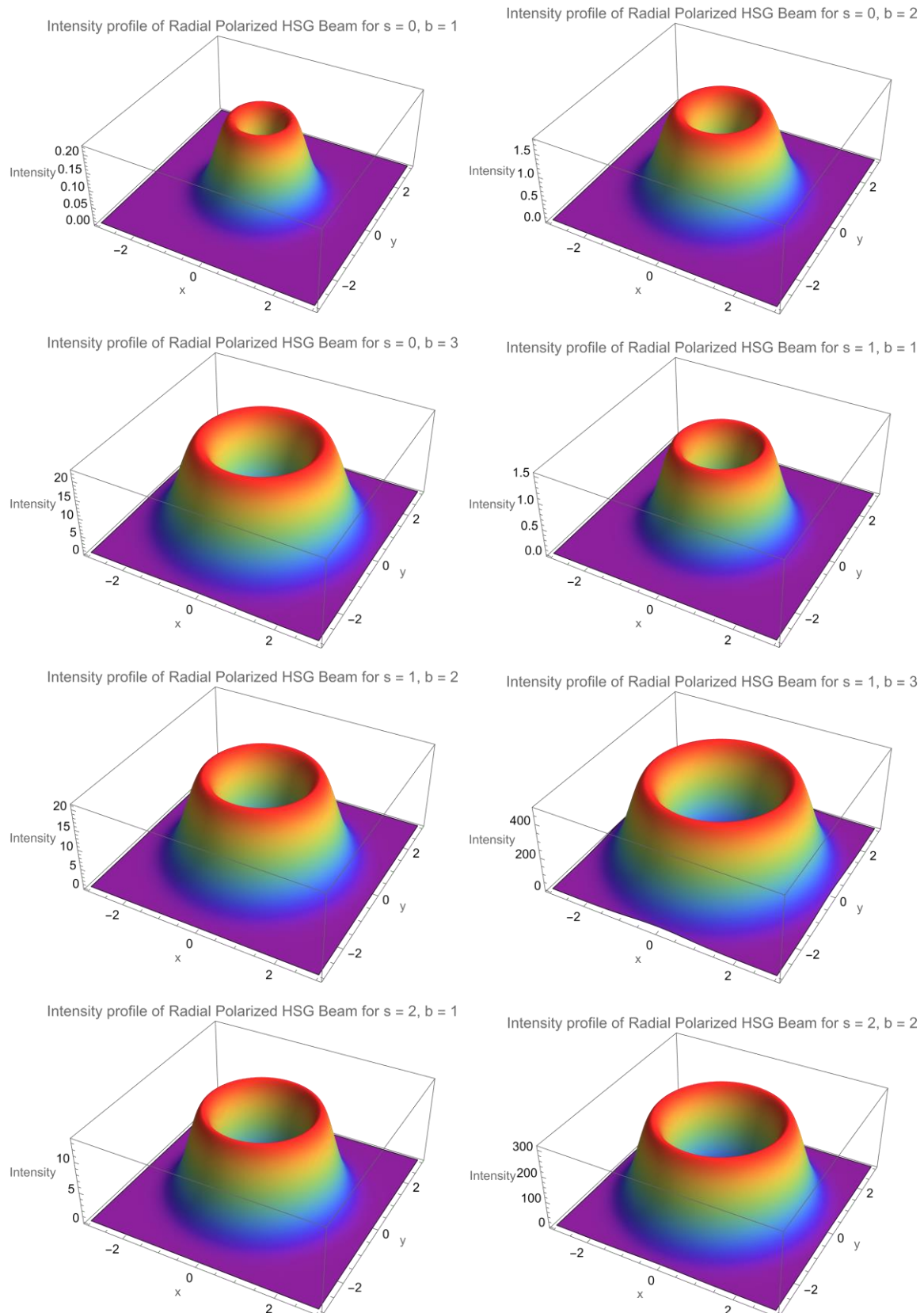


Figure 1. Intensity profile of Hermite-Sinh-Gaussian laser pulse for various $s = 0,1,2$ and $b = 1,2,3$ values.

$$\text{Here, } c_2 = \frac{1}{\sqrt{1-\beta_z^2}} + \frac{\beta_z^2}{(1-\beta_z^2)^{3/2}}$$

From equation (8)

$$\frac{d\beta_\theta}{dt'} = 0 \quad (13)$$

Equation (10) to (13) are the coupled differential equations, which can be solved for feasible numerical values of the parameters.

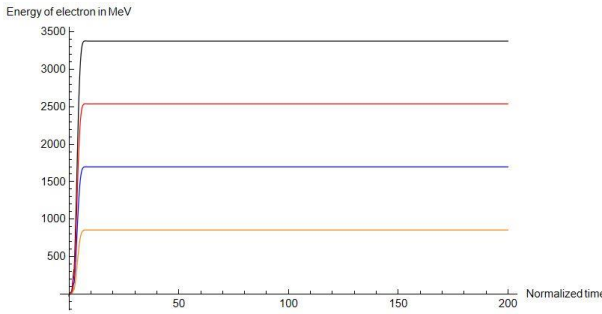


Figure 2. Variation of energy of electron with normalized time for normalized laser electric field of 5 (orange), 10 (blue), 15 (red) and 20 (black), $b = 3$, $s = 2$, $r'_0 = 2$, $\lambda = 1.06 \mu\text{m}$.

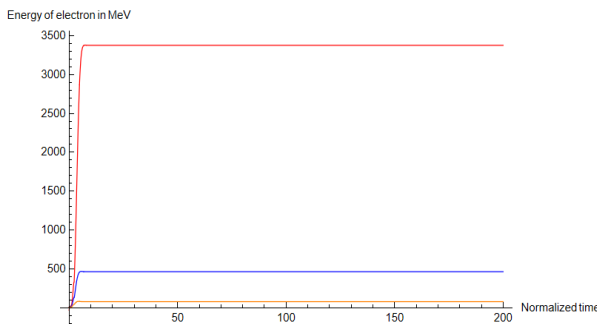


Figure 3. Variation of energy of electron with normalized time for decentred parameter of 1 (orange), 2 (blue), and 3 (red), $a_0 = 20$, $s = 2$, $r'_0 = 2$, $\lambda = 1.06 \mu\text{m}$.

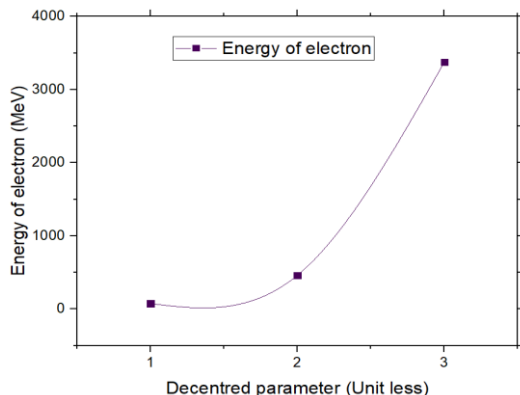


Figure 4. Variation of energy of electron with decentred parameter for $t' = 200$, $a_0 = 20$, $s = 2$, $r'_0 = 2$, $\lambda = 1.06 \mu\text{m}$

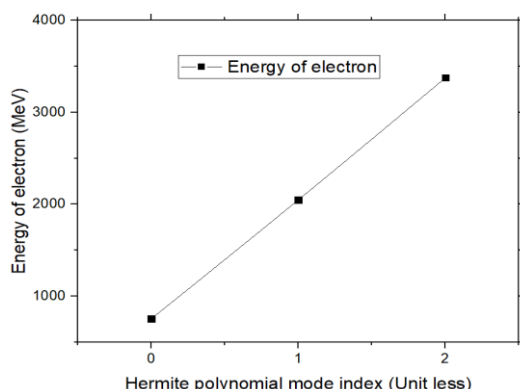


Figure 5. Variation of energy of electron with Hermite polynomial mode index for $t' = 200$, $a_0 = 20$, $b = 3$, $r'_0 = 2$, $\lambda = 10.6 \mu\text{m}$.

3. Results and discussion

For numerical solutions, laser of wavelength $1.06 \mu\text{m}$ is chosen (Nd: YAG laser). The angular frequency ω for the selected wavelength is 1.78×10^{15} rad/sec. The normalized values of laser electric field amplitude a_0 is chosen as 5, 10, 15 and 20 which correspond to laser electric field of 1.5×10^{13} , 3×10^{13} , 4.5×10^{13} and 6×10^{13} V/m. Laser intensity for the chosen electric field is 3×10^{19} , 1.2×10^{20} , 2.75×10^{20} and 4.89×10^{20} W/cm^2 . Hermite polynomial mode index (s) is chosen as 0, 1 and 2. Decentered parameter (b) for the sinh function is chosen as 1, 2 and 3. Normalized value of beam waist is chosen as 2. We have taken initial normalized radial position of electron at 0.1 moving along radial direction with energy 0.25 MeV.

Effect of laser electric field amplitude

The energy of an electron in a vacuum increase with the normalized amplitude (a) of the electric field of a laser. For $a = 5, 10, 15$, and 20, the associated maximum electron energies are 854.32 MeV, 1696.80 MeV, 2536.84 MeV, and 3375.75 MeV, respectively. This variation is shown in figure 2. This pattern indicates a clear correlation that electron energy increases linearly with the electric field amplitude. Increased electric field amplitudes lead to enhanced electron acceleration owing to a more robust interaction with the laser field. These results emphasized the capability of high-intensity lasers to generate ultra-relativistic electrons, applicable in sophisticated light sources and high-energy physics.

Effect of decentred parameter

The research indicates that the energy of an electron in a vacuum markedly escalates with the decentred parameter b of the sinh function, which adjusts the amplitude of the laser electric field. At $b=1$, the electron energy is 76.09 MeV, which increases to 462.42 MeV at $b=2$, and attains 3375.75 MeV at $b=3$ as shown in figure 3. With increase in decentred parameter, the maximum intensity as well as the central hollow region of HSG profile increases as shown in figure 1. This illustrates a non-linear correlation between b and electron energy, ascribed to the augmented interaction between the electron and the laser field with increasing b.

The decentred parameter b alters the spatial distribution of the electric field defined by the sinh function. As b grows, the peak intensity of the field becomes more prominent due to exponential growth of the sinh function, leading to a greater electric field amplitude which creates a dramatic rise (nonlinear increase) in the energy imparted to the electron as b increases as shown in figure 4.

Effect of Hermite polynomial mode index

Hermite polynomials define the spatial distribution of modes in HSG laser pulses. The mode index characterizes the number of nodes in the transverse electric field distribution. The findings indicate a substantial rise in the electron's energy as s escalates: $s=0$: Energy equals 754.87 MeV, Energy escalates to 2047.75 MeV, representing an increase of almost 2.7 times. At $s=2$, energy attains 3375.75 MeV, representing an

increase of about 1.6 times from $s=1$. The nonlinear rise indicates that elevated mode indices improve interaction efficiency by generating more robust and organized electromagnetic fields, resulting in linearly enhanced energy transfer to the electron.

The energy acquired by an electron interacting with a laser pulse in a vacuum is contingent upon the intensity, and spatial configuration of the laser field. In HSG laser pulses, higher mode indices enhance the peak intensity and electric field gradients inside the interaction zone. The electron undergoes more acceleration owing to the heightened electric field intensity and spatial configuration.

In a study, Sharma et al. [19] mainly focused on the effect of linear chirping parameters. With the increase of positive frequency chirp, the maximum energy of the electron decreases while increase in negative frequency chirp enhances electron energy. A maximum energy gain of 3738.3 MeV was obtained with a frequency chirp of -0.0099 . Sharma et al. [20] have investigated electron acceleration in vacuum using sinh-Gaussian laser pulse and they obtained electrons of 1.21 GeV energy with optimized laser parameters (decentered parameter $b = 3$, $\lambda = 1.06 \mu\text{m}$). In this study, we have utilized Hermite-sinh-Gaussian laser pulse to obtain 3.37 GeV electrons (decentered parameter $b = 3$, $s = 2$, $\lambda = 1.06 \mu\text{m}$). The HSG pulse, characterized by a Hermite mode index of 2 ($H_2(x) = 4x^2 - 2$), creates stronger transverse intensity gradients due to its more complex beam profile. The fundamental distinction between the acceleration of electrons by means of Sinh-Gaussian laser and Hermite-sinh-Gaussian functions lies in the incorporation of the Hermite function. As the indexes of higher Hermite polynomial modes and the parameters of greater decentering are considered, there is an observable increase in laser intensity within regions of elevated transverse distance. This phenomenon can be attributed to the contributions of both the sinh function and the Hermite functions. By optimizing the parameters, a

maximum energy gain of 3375.75 MeV electron can be obtained without any chirping. This results in the establishment of conditions that are more conducive for electrons to absorb increased amounts of energy.

4. Conclusion

The research shows that Hermite-sinh-Gaussian (HSG) laser beams may boost vacuum electron acceleration. Using HSG beams' hybrid structure, which combines Hermite-Gaussian orthogonality with non-Gaussian characteristics from the hyperbolic sine (sinh) function, the research highlights the role of key parameters like the Hermite mode index (s), decentered parameter (b), and electric field amplitude and distribution. Optimizations (e.g., $s=2$, $b=3$) may produce energy increases of 3375.75 MeV, according to theoretical modelling and numerical simulations. This study provides light on beam characteristics and electron acceleration dynamics, paving the door for small, high-efficiency laser-driven particle accelerators.

Declarations

Funding

Not applicable

Ethics approval

Not applicable

Consent to participate.

Not applicable

Consent for Publication

Not applicable

Conflict of Interest

The authors declare no competing interest.

Author Contribution: Vivek Sharma: derivation, methodology, analytical modeling, graph plotting; Vishal Thakur: supervision, reviewing, and editing.

Data Availability:

The data that supports the findings of this study are available from the corresponding authors upon reasonable request.

References

1. A Varma, A Kumar, *Optik (Stuttg)* **228** (2021).
2. A Varma, S P Mishra, A Kumar, A Kumar, *Laser Phys Lett* **20** (2023).
3. H S Ghotra, N Kant, *Laser and Particle Beams* **34** (2016).
4. E J Bochov, G T Moore, M O Scully, *Phys Rev A* **46** (1992).
5. M Martyanov et al., *High Power Laser Science and Engineering* **11** (2023).
6. N Kant, V Thakur, *Opt Quantum Electron* **53** (2021).
7. H K Midha, V Sharma, N Kant, V Thakur, *Journal of Optics* (2024).
8. M Hashemzadeh, *Brazilian Journal of Physics* **53** (2023).
9. A K Pramanik, H S Ghotra, N. Kant, J. Rajput, *Laser Phys Lett* **19** (2022).
10. H K Midha, V Sharma, N Kant, V Thakur, *Applied Physics B* **130** (2024).
11. Z Liu, X Wang, K Hang, *Sci Rep* **9** (2019).
12. S Konar, S Jana, *Opt Commun* **236** (2004).
13. K Tian, X Xia, *Laser and Particle Beams* (2022).
14. N Gupta, R Johari, *J Appl Spectrosc* **90** (2023).
15. K P Singh, D N Gupta, V Sajal, *Laser and Particle Beams* **27** (2009).
16. A K Pramanik, H S Ghotra, J Rajput, *The European Physical Journal D* **77** (2023).
17. J Singh, J Rajput, H S Ghotra, N Kant, *Commun Theor Phys* **73** (2021).
18. H Akou, A S Firouzjaei, *Phys Plasmas* **27** (2020).

19. V Sharma, V Thakur, *Journal of Optics* (2025).
20. V Sharma, R Kaur, V Thakur, *Journal of Optics* (2024).